

## Control over Phase Curvature Using Mixtures of Polymerizable Surfactants

Julian Eastoe\* and Mark Summers

*School of Chemistry, University of Bristol,  
Bristol BS8 1TS, United Kingdom*

Richard K. Heenan

*ISIS-CLRC, Rutherford Appleton Laboratory,  
Chilton, OXON OX11 0QX, United Kingdom*

Received May 26, 2000

Revised Manuscript Received September 19, 2000

A central theme in modern materials chemistry is the template-directed fabrication of nanostructured architectures. Reactive surfactant monomers (surfmers) have been successfully employed to polymerize aqueous micelles (e.g., refs 1–5), vesicles (e.g., refs 6 and 7), lyotropic liquid crystals (e.g., refs 8–14), and microemulsions (e.g., ref 15). The general aim is to obtain robust nanostructured reaction media for preparing a range of systems such as MCM materials,<sup>16</sup> polymer nanocomposites,<sup>17</sup> encapsulated metals,<sup>18</sup> high surface area catalysts,<sup>19</sup> and electrodes.<sup>20</sup> There are a number of excellent reviews and the reader is referred to refs 21–23 for more comprehensive literature coverage. In

all of the work published to date, a single surfactant has been used and this enforces limitations on the interfacial curvature, and phase structure, which can be achieved in both the initial and the final polymerized states. A new approach is taken here with two chemically pure single- and double-chained surfactants, as shown in Figure 1. By mixing these surfmers at well-defined compositions, it is possible to control the preferred curvature of the nonpolymerized system. Interestingly, direct structural evidence from small-angle neutron scattering (SANS) and polarizing light microscopy (PLM) indicates that after free-radical polymerization, both in aqueous micelles and lyotropic liquid crystals, the phase structures are broadly retained. These new results demonstrate the general utility of surfmer mixtures to achieve a desired curvature.

To understand self-assembly structures with surfactants, it is helpful to consider a packing parameter,  $P$ , which is the ratio of hydrophobic chain volume,  $V$ , to an effective volume occupied per molecule in the aggregate,  $V_{\text{eff}}$ .<sup>24</sup> Aggregate shape changes occur at critical values of  $P$ ,<sup>24</sup> and changes in  $V$ , and/or the effective molecular area,  $a_{\text{eff}}$ , can drive transitions. With a single surfactant,  $V$  is essentially constant and  $a_{\text{eff}}$  is controlled principally by headgroup interactions; hence, there is only limited scope for changing  $P$  to achieve different structures. On the other hand, with appropriate mixtures of single-, double- (and triple-) chain compounds, virtually all curvatures may be accessed. For example, the nonreactive  $C_{12}$  cationic dodecyltrimethylammonium bromide (DTAB, single chain) and di-dodecyl dimethylammonium bromide (DDAB, double chain) have  $P$  values of 0.33 and 0.62;<sup>25</sup> hence, curvature of a mixture of can be changed between the two limits, depending on the composition. Mixtures of DDAB and DTAB have been used to demonstrate how preferred curvature can be controlled by composition, both in aqueous micelles and microemulsions.<sup>26,27</sup> In a similar fashion, with mixtures of appropriate reactive surfactants, it should also be possible to select curvature, from normal spherical micelles in water, through to reversed spherical micelles in oil. Here are described preliminary results on aqueous systems formed by the mixtures of the two surfmers **A** and **B** (Figure 1). This is a flexible approach with much potential for expanding the scope and applications of polymerized surfactant phases. Returning to the nonreactive analogues DTAB and DDAB, it was shown that mixing in the micelles is ideal,<sup>26</sup> and

\* To whom correspondence should be addressed. E-mail: julian.eastoe@bristol.ac.uk. Tel.: +117 9289180. Fax: +117 9250612.

- (1) Fendler, J. F.; Tundo, P. *Acc. Chem. Res.* **1984**, *17*, 3.
- (2) Paleos, C. M.; Dais, P.; Malliaris, A. *J. Polym. Sci. Polym. Chem. Ed.* **1984**, *22*, 3383.
- (3) Hamid, S. M.; Sherrington, D. C. *Polymer* **1987**, *28*, 332.
- (4) Kline, S. R. *Langmuir* **1999**, *15*, 2726.
- (5) Bütün, V.; Wang, X.-S.; de Paz Bññez, M. V.; Robinson, K. L.; Billingham, N. C.; Armes, S. P.; Tuzar, Z. *Macromolecules* **2000**, *33*, 1.
- (6) Regen, S. L.; Czech, B.; Singh, A. *J. Am. Chem. Soc.* **1980**, *102*, 6638.
- (7) Jung, M.; Der Ouden, I.; Montoya-Goñi, A.; Hubert, D. H. W.; Frederik, P. M.; van Herk, A. M.; German, A. L. *Langmuir* **2000**, *16*, 4185.
- (8) Thundathil, R.; Stoffer, J. O.; Friberg, S. E. *J. Polym. Sci. Polym. Chem. Ed.* **1980**, *18*, 2629.
- (9) Micas, J.; Paleos, C. M.; Dais, P. *Liq. Cryst.* **1989**, *5*, 1737.
- (10) McGrath, K. M. *Colloid Polym. Sci.* **1996**, *274*, 399. McGrath, K. M.; Drummond, C. J. *Colloid Polym. Sci.* **1996**, *274*, 316 and 612.
- (11) Srisiri, W.; Sisson, T. M.; O'Brien, D. F.; Mc. Grath, K. M.; Han, Y.; Gruner, S. M. *J. Am. Chem. Soc.* **1997**, *119*, 4866.
- (12) Srisiri, W.; Lee, Y. S.; Sisson, T. M.; Bondurant, B.; O'Brien, D. F. *Tetrahedron* **1997**, *53*, 15397.
- (13) Sisson, T. M.; Srisiri, W.; O'Brien, D. F. *J. Am. Chem. Soc.* **1998**, *120*, 2322.
- (14) Rodríguez, J. F.; Soltero, J. F. A.; Puig, J. E.; Schulz, P. C.; Espinoza-Martínez, M. L.; Pieroni, O. *Colloid Polym. Sci.* **1999**, *277*, 1215.
- (15) Pawlowski, D.; Haibel, A.; Tieke, B. *Ber. Bunsen-Ges. Phys. Chem.* **1998**, *102*, 1865.
- (16) Dreja, M.; Pyckhout-Hintzen, W.; Tieke, B. *Macromolecules* **1998**, *31*, 272.
- (17) Khulashalani, D.; Kuperman, A.; Coombs, N.; Ozin, G. A. *Chem. Mater.* **1996**, *8*, 2188.
- (18) Smith, R. C.; Fischer, W. M.; Gin, D. L. *J. Am. Chem. Soc.* **1997**, *119*, 4092.
- (19) Deng, H.; Gin, D. L.; Smith, R. C. *J. Am. Chem. Soc.* **1987**, *109*, 3522.
- (20) Ding, J. H.; Gin, D. L. *Chem. Mater.* **2000**, *12*, 22.
- (21) Elliott, M.; Birkin, P. R.; Bartlett P. N.; Attard, G. S. *Langmuir* **1999**, *15*, 7411.
- (22) Armitage, B. A.; Bennett, D. E.; Lamparski, H. G.; O'Brien, D. F. *Adv. Polym. Sci.* **1996**, *126*, 53.
- (23) Guyot, A. *Curr. Opin. Colloid Interface Sci.* **1996**, *5*, 580.

(23) Guyot, A. *Novel Surfactants*; Marcel Dekker: New York, 1998; p 301.

(24) Israelachvili, J. *Intermolecular and Surface Forces*; Academic Press: New York, 1992. If the surfactant chain length is  $l$  and the effective area per molecule at the aggregate surface is  $a_{\text{eff}}$ , then  $P = V/(a_{\text{eff}}l)$ . For  $P < 1/3$  spherical micelles are present; for  $1/3 < P < 1/2$  cylinders are preferred; for  $1/2 < P < 1$  flexible bilayers are favored, while for  $P > 1$  reverse micelles form. This also introduces the concept of film curvature: in aqueous systems curvature is defined as positive and  $P < 1$ , whereas for oil-continuous systems curvature is negative and  $P > 1$ .

(25) Warr, G. G.; Sen, R.; Evans, D. F.; Trend, J. F. *J. Phys. Chem.* **1988**, *92*, 774.

(26) Lusvardi, K. M.; Full, A. P.; Kaler, E. W. *Langmuir* **1995**, *11*, 487.

(27) Bumajdad, A.; Eastoe, J.; Griffiths, P.; Steytler, D. C.; Heenan, R. K.; Lu, J. R.; Timmins, P. *Langmuir* **1999**, *15*, 5271.

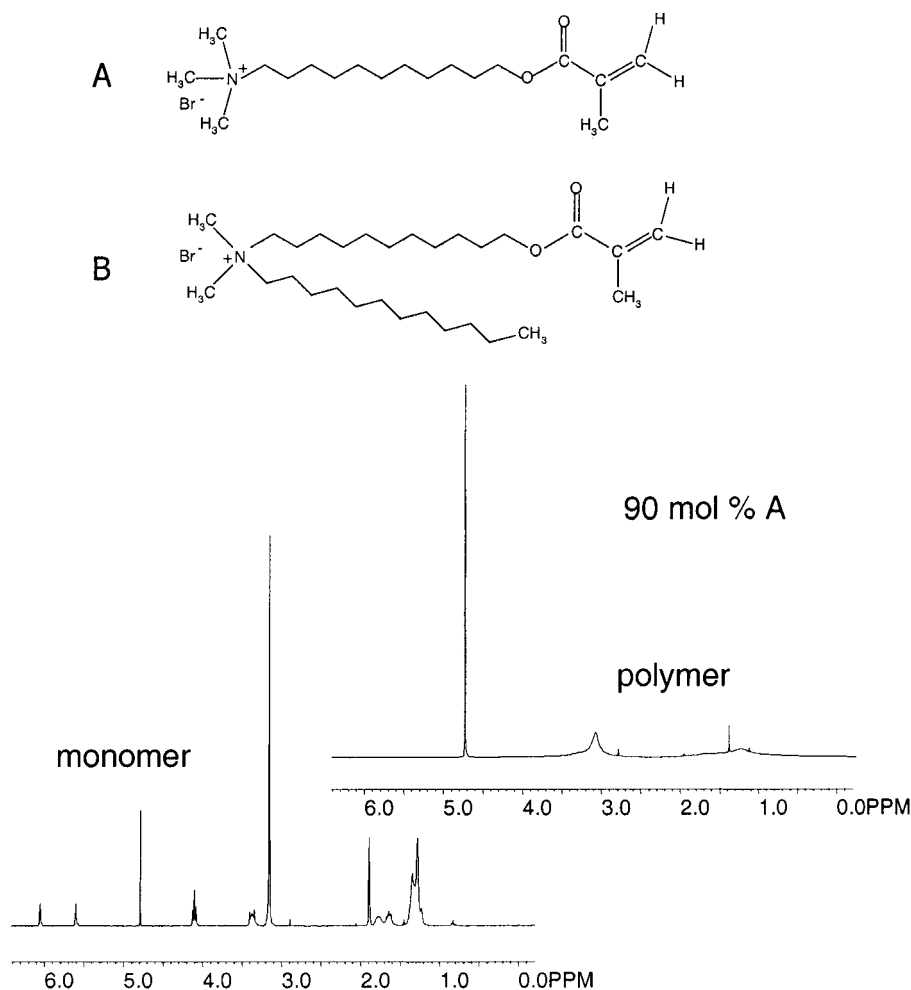


**Figure 1.** Chemical structures of the surfmers **A** (11-(methacryloyloxy)undecyltrimethylammonium bromide) and **B** (dodecyl(11-(methacryloyloxy)undecyl)dimethylammonium bromide). Example 300 MHz <sup>1</sup>H NMR spectra at 298 K for micelles in D<sub>2</sub>O formed by a 9:1 mixture of **A**:**B** on a mole basis, before and after the polymerization.

in water-in-oil microemulsions both surfactants are strongly bound and randomly mixed at the interface.<sup>27</sup> Therefore, owing to the structural similarity, it can be expected that surfmers **A** and **B** are also evenly distributed within mixed micelles and surface films.

The precursor common to both surfmers, bromoundecyl methacrylate, was made as given in ref 9. The single-chain **A**, 11-(methacryloyloxy)undecyltrimethylammonium bromide, was synthesized as described before.<sup>9</sup> Reagents and solvents 11-bromo-1-undecanol (98%), anhydrous pyridine (99.8%), THF (99.9%) (all from Aldrich), methacryloyl chloride (97%), 4-methoxyphenol (98+% both from Lancaster), and trimethylamine (99% Fluka) were used as supplied. The di-chain **B**, dodecyl(11-(methacryloyloxy)undecyl)dimethylammonium bromide was prepared by reacting a 1:1.05 molar ratio of bromoundecyl methacrylate to *N,N*-dimethyldodecylamine (97% Aldrich), in the presence of an inhibitor, in ethanol. The reaction mixture was refluxed for 6 h, the solvent was then removed, and crystals of **B** were washed with ether, filtered, and dried. NMR (JEOL Lambda 300), mass spectroscopy (VG Analytical Autospec), and elemental analysis established the chemical structures of bromoundecyl methacrylate and the surfmers **A** and **B**. Samples were made up in D<sub>2</sub>O Fluorochem Limited (purity 99.9%) in terms

of the total surfmer concentration and the mol % of **A** and **B**, and heated in sealed vials to ensure complete homogenization. Polymerizations were initiated by 2,2'-azobis(2-methylpropanamide) dihydrochloride (Aldrich 97%), and the samples were heated to 60 °C for 2 h. The macroscopic appearance of the samples changed little, although in general polymerized systems they were of slightly higher viscosity. The reaction was monitored by the disappearance of vinyl signals in the NMR spectra (e.g., Figure 1). SANS experiments were carried out on LOQ (at ISIS, UK) to determine the absolute scattering intensity,  $I(Q)$  (cm<sup>-1</sup>), as fully described elsewhere.<sup>28,29</sup> (Note the same samples were studied by both NMR and SANS). The SANS data for the "before" and "after" polymerization cases were modeled using a least-squares fitting package to obtain information on aggregate dimensions.<sup>30</sup> Polarizing light microscopy (Nikon Optiphot 1 and Linkam heating-

(28) Heenan, R. K.; King S. M.; Penfold, J. *J. Appl. Cryst.* **1997**, *30*, 1140.

(29) The solutions were made up in D<sub>2</sub>O so as to contrast the entire *h*-surfmer aggregate, and samples were thermostated in 2-mm path length cuvettes at 25 ± 0.2 °C.

(30) Heenan, R. K. *FISH Data Analysis Program*; Rutherford Appleton Laboratory Report RAL-89-129; CCLRC: Didcot, UK, 1989. Hayter, J. B.; Penfold, J. *Mol. Phys.* **1981**, *42*, 109. Hayter, J. B.; Penfold, J. *J. Chem. Soc. Faraday Trans. 1* **1981**, *77*, 1851.

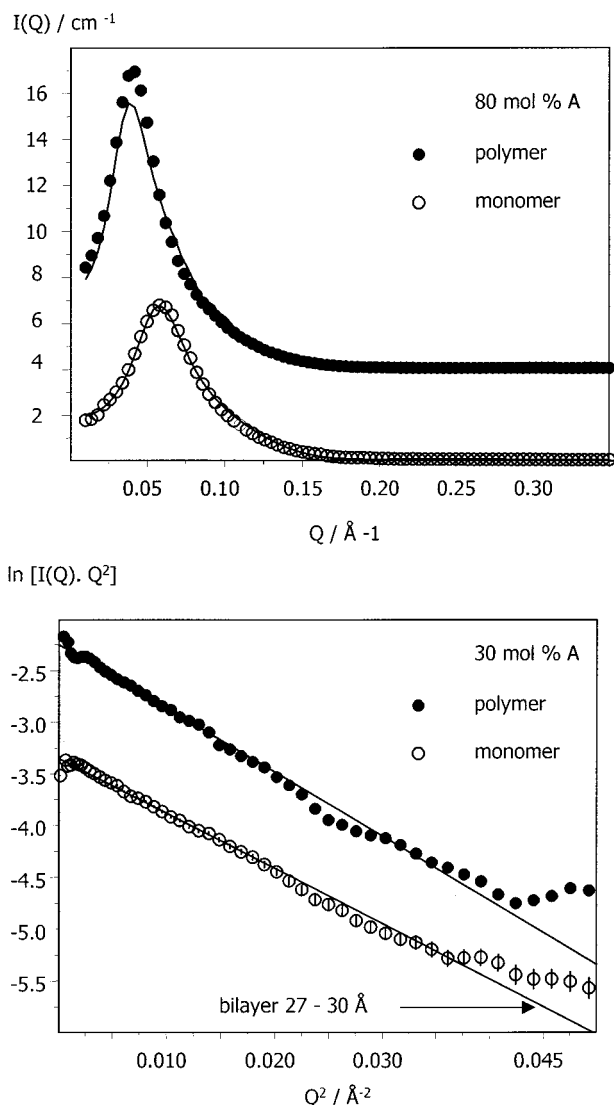


**Figure 2.** Example SANS data and model fits (lines) for two different mixing ratios before and after polymerization. The curves for polymerized samples have been shifted upward by a constant for clarity of presentation. Total surfmer concentration = 0.15 mol dm<sup>-3</sup>.

cooling stage) was used to determine the lyotropic optical textures as a function of composition and polymerization.

As shown in Figure 1, the NMR spectra are consistent with the formation of a polymer after the reaction. Comparison of the integrated <sup>1</sup>H NMR peaks indicates a loss of the vinyl ( $\delta = 6.10, 5.55$ ) with respect to the quaternary ammonium methyl protons ( $\delta = 3.4, 3.46$ ) and essentially 100% conversion. (HOD appears at  $\delta \sim 4.7-4.8$ ). Furthermore, line broadening owing to more efficient relaxation is observed in the polymer. These observations are similar to those seen before with related pure single-chain surfmers (e.g., ref 3).

SANS is an ideal, direct method for investigating micelles because the hydrocarbon surfactant can be contrasted by using D<sub>2</sub>O, and for a given structure the scattering intensity reports on the particle number density. Therefore, any changes in structure and concentration owing to polymerization can be readily ascertained. Figure 2 shows example SANS curves for **A** at 80 and 30 mol % of the total surfactant present.

**Table 1. Parameters Obtained from Analysis of SANS Data from Dilute Aqueous Phases<sup>a</sup>**

mol % A	micelle structure	D / Å	
100 np	spherical	20.8	
100 p		23.8	
90 np		21.0	
90 p		24.7	
80 np		23.1	
80 p		26.3	
70 np		26.1	
70 p		27.0	
60 np		25.6	
60 p		26.0	
50 np	cylindrical	25.4	
50 p		$I(Q) \sim Q^{-1}$	20.5
40 np		disc	26.6
40 p		$I(Q) \sim Q^{-2}$	28.2
30 np			26.2
30 p			28.0
20 np			25.7
20 p			27.9

<sup>a</sup> "np" denotes nonpolymerized (monomer) and "p" the polymerized system. Total surfactant concentration = 0.15 mol dm<sup>-3</sup>. The characteristic dimension, *D*, corresponds to the sphere radius, cylinder radius, and bilayer thickness, respectively. The uncertainty on *D* is  $\pm 2.5$  Å.

The relative intensities for "before" and "after" samples indicate no significant change in the micelle concentrations. The parameters obtained from extensive model fitting are given in Table 1. Between 100 and 60 mol % **A** the SANS curves were characteristic of charged spherical micelles, with a strong repulsive structure factor,  $S(Q)$ , such as that shown in the top panel of Figure 2. These data were fitted using the usual Hayter Penfold model, resulting in a charge per molecule of 0.2–0.3, which is typical of micelles of a 1:1 ionic surfactant.<sup>30</sup> The micelle radii, in the region of 23 Å, are similar to those for a C12-chain surfactant, such as anionic SDS.<sup>30</sup> As can be seen in Figure 2, SANS curves for the monomer and polymer systems are very similar, although model fitting indicates the radius seems to be slightly larger in the polymer (Table 1, and small shift to lower *Q* of the maximum). Therefore, the counterion binding and micellar surface are hardly affected by cross-linking of the hydrophobic ends. Under certain conditions SANS is useful for detecting micelle shape changes, such as sphere  $\rightarrow$  rod  $\rightarrow$  disk.<sup>31</sup> At 50 mol % surfmer **A** the SANS shows a region of  $Q^{-1}$  decay, while at higher percentages of double-chain **B** intensity  $\propto Q^{-2}$  across a wide *Q* range. A good way to discriminate between different shapes is via the Guinier law,  $I(Q) \propto Q^{-x} \exp(-R_g^2 Q^2/3)$ , where  $x = 1$  for rods and 2 for disks and the radius of gyration,  $R_g$ , is related to the appropriate cross-section dimension.<sup>31</sup> The lower panel of Figure 2 shows this, for examples with 30 mol % **A**, such that the linear decay is indicative of bilayers of the order of 27-Å-thick for both the monomeric and polymerized systems (any differences are within the uncertainties). Note that the all-trans C12 chain length is around 16 Å, so these dimensions are consistent with bilayers.

Because SANS and NMR show that the free and polymerized micelles have very similar structures, it is of interest to see how these surfmers behave in more

(31) For cylinders there is a region of logarithmic decay,  $I(Q) \sim Q^{-1}$ , whereas for sheetlike structures there is switch over to a  $Q^{-2}$  power law. See Eastoe, J. *New Physico-Chemical Techniques for the Characterisation of Complex Food Systems*; Dickenson, E., Ed.; Blackie: Glasgow, 1995; p 268.

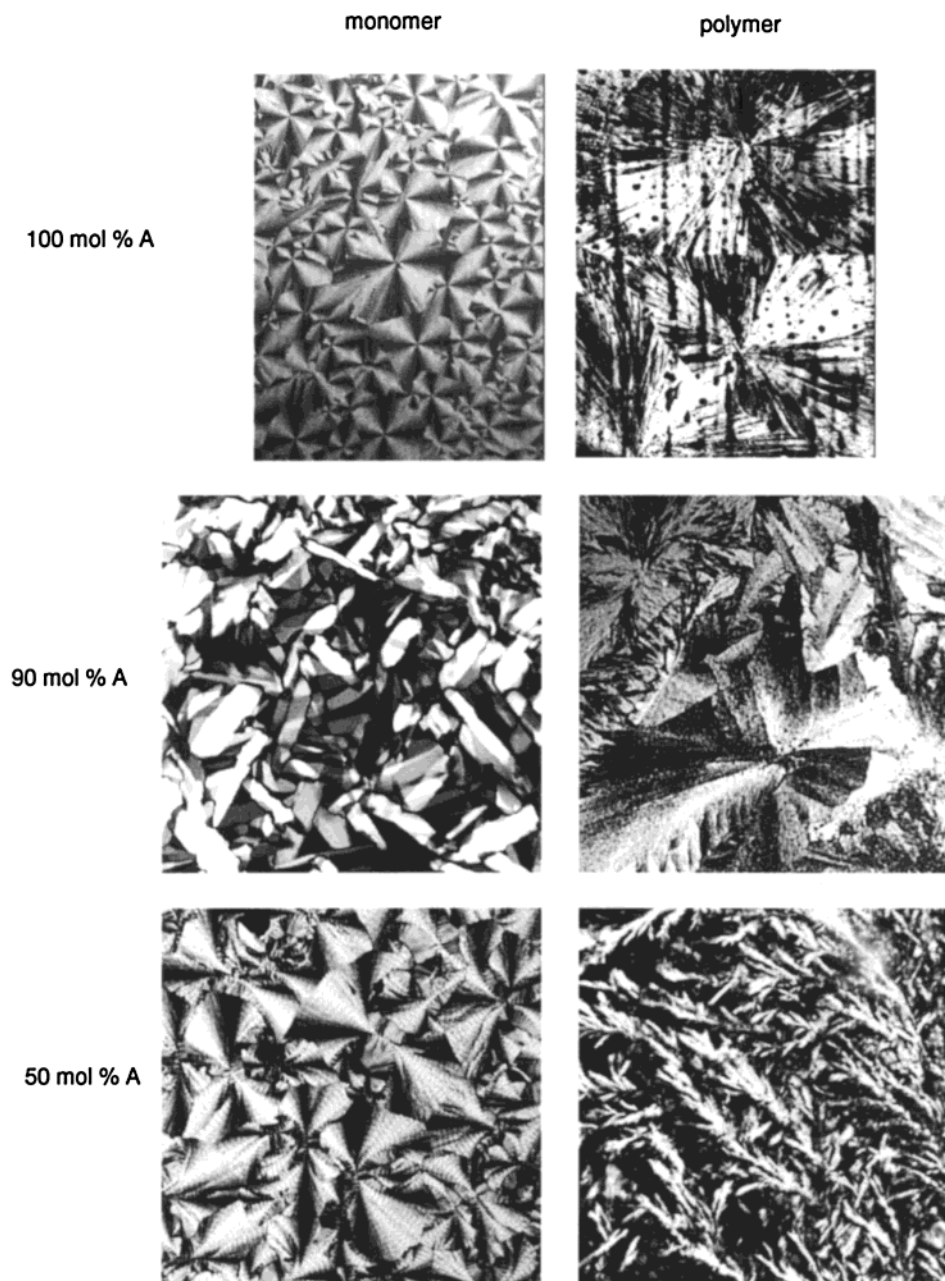


**Figure 3.** Example optical textures for three different mixing ratios before and after polymerization. Samples with 100 and 90 mol % **A** are at 40% total surfactant mass. The systems at 50 mol % **A** – 50 mol % **B** are at 90% total surfactant mass.

concentrated lyotropic mesophases. Polarizing light microscopy (PLM) is a convenient method for assessing liquid-crystalline phase behavior, and examples of optical textures are given elsewhere.<sup>32</sup> Figure 3 shows PLM textures before and after polymerization.<sup>33</sup> The samples with 100 mol % **A** and 90 mol % **A** + 10 mol % **B** are at 40% by mass of total surfactant. The sample with 100% **A** exhibits a classic “fan” texture of  $H_1$ , while the 90 mol % **A** system displays a “batonnet” pattern.<sup>32</sup> These pictures indicate that hexagonal phases are retained, suggesting other polymerized phases can be prepared in a similar way. On the basis of estimates for relative packing fractions of the two surfactants, a lamellar

phase should dominate for mixtures below  $\approx 65$  mol % **A**. The mixture with 50 mol % **A** + 50 mol % **B**, but at 90% total surfactant, possesses a “focal conic” texture, which may be attributed to  $L_{\alpha}$ .<sup>32</sup> In other words, the phase structure responds in a predictable way to variation in both mixture composition and total surfactant concentration. These PLM images are at the same magnification, and it is interesting to note an increase in mean domain size with the polymerized samples.

The polymerization of the single-chain **A**, and related surfactants, has been investigated before, and the main conclusion was that the reaction produced a “polysoap” rather than a truly “polymerized micelle”.<sup>3</sup> Results from vapor pressure osmometry suggested a typical degree of polymerization of about 25.<sup>3</sup> Our direct SANS studies suggest that the overall aggregate size does not change (much), and hence the average number of monomer units per cluster remains essentially constant. However,

(32) Laughlin, R. G. *The Aqueous Phase Behaviour of Surfactants*; Academic Press: London, 1994.

(33) The reaction was initiated in the fluid micellar phase, and the lyotropic mesophases were prepared gravimetrically by controlled evaporation of water.

we are not in a position to say whether these aggregates are "polysoaps", "polymerized micelles", or a mixture of the two. In conclusion, the composition of a mixed system consisting of single- and double-chain reactive surfactants can be used to control curvature of nonpolymerized and cross-linked phases.

**Acknowledgment.** M.S. acknowledges the support of EPSRC in terms of a Quota studentship. We also thank CLRC for allocation of beam time at ISIS and a grant toward consumables and travel.

CM001096Z